

Prediction of Fast Fading Mobile Radio Channels in Wideband Communication Systems

Liang Dong, Guanghan Xu and Hao Ling
Department of Electrical and Computer Engineering
The University of Texas, Austin, TX 78712

Abstract—The fast fading mobile radio channels place fundamental limitations on the performance of wireless communication systems, such that the prediction of the changing channel behaviors is of interest. For the frequency-selective fading channels in wideband systems, the knowledge of the channel transfer function over the entire frequency band is required. In this paper, we propose an ESPRIT-type algorithm to model and further predict the wideband time-varying channel at different frequencies jointly, assuming that the scatterers remain constant. Simulation results show that the joint-frequency prediction scheme has superior performance over conducting the channel prediction on a single frequency.

I. INTRODUCTION

The radio channel in a wireless communication system is often characterized by multipath propagation. A fading signal results from interference between multipath components at the receiver. For transceivers moving at high speeds, the channel varies dramatically and undergoes deep fades within a typical time frame of several milliseconds. Future mobile systems will use higher carrier frequencies, with associated higher fading rates. Since the channel changes rapidly, usually the transceivers are not optimized for current channel conditions and thus fail to exploit the full potential of the wireless channels. To improve the system performance, adaptive transmission techniques are applied to combat the fast fading channel effect. To realize the potential of adaptive transmission methods, fading channel variations have to be reliably predicted at least several milliseconds ahead [1].

Recently, researchers have speculated that the fading process is in fact a deterministic sinusoidal

process with time-varying parameters, and can be characterized using a discrete scatter propagation model [2]. Spectral estimation followed by linear prediction and interpolation is applied in [3] and [1] to predict the evolution of the channel. This algorithm characterizes the fading channel using an autoregressive (AR) model. Subspace-based methods are also used to predict the channel. A modified root-MUSIC algorithm is used in [4], and an ESPRIT algorithm is used in [5] to estimate the dominant sinusoids that make up the fading channel. Then these sinusoids are extrapolated to predict future channel samples. These algorithms predict the fading channels encountered in narrowband mobile communication systems. In [6], the statistical dependencies in sequences of wideband mobile radio channel data are measured, and a nonlinear model is used for the fading channel prediction.

In this paper, we propose an ESPRIT-type [7] algorithm to predict the frequency-selective channel in wideband systems. The time-varying channel transfer function at different frequencies within the wideband are modeled and predicted jointly. Simulation results demonstrate that the performance of the proposed prediction algorithm is better than processing channel prediction on each frequency separately.

II. WIDEBAND CHANNEL MODEL

The baseband equivalent channel between the base station (BS) and the mobile is modeled using the time-varying impulse response

$$h(\tau; t) = \sum_{k=1}^L \beta_k(t) \delta(\tau - \tau_k) \quad (1)$$

where L is the total number of multipaths from discrete scatterers. The variable t indicates the time-varying property, and τ is the delay variable. β_k and τ_k are the complex amplitude and path delay of the k^{th} multipath component, respectively.

Due to the motion of the mobile or the scatterers, the BS received signals experience Doppler frequency spread. The increased mobility results in fast fading in which the channel exhibits rapid temporal variations, such that the performance of the cellular radio system is substantially degraded. Fast-fading channels encountered in practice exhibit Doppler spreads on the order of 100-200 Hz. At higher and higher carrier frequencies of new generation wireless systems, the radio channel will vary dramatically within a typical data frame of several milliseconds. The complex amplitude $\beta_k(t)$ can be expressed as

$$\beta_k(t) = \alpha_k e^{j(2\pi f_k t + \phi_k)} \quad (2)$$

where α_k , f_k , ϕ_k are the path loss, Doppler frequency shift and phase offset of the k^{th} multipath component, respectively. The Doppler frequency is given by $f_k = f_c \frac{v}{c} \cos(\theta_k)$, where f_c is the carrier frequency, v is the speed of the mobile, c is the speed of light, and θ_k is the angle between the k^{th} mobile incident ray and the mobile moving direction. The fading channel varies rapidly with increases in mobile speed. We assume a far-field condition, where the path loss and the phase offset remain constant during the short time of the channel analysis and prediction range. At carrier frequencies as high as several giga-hertz, typical motion of the mobile may be linearized over distances of several wavelengths.

The channel transfer function which is the Fourier transform of the channel impulse response on the argument τ is

$$H(f; t) = \sum_{k=1}^L \beta_k(t) e^{-j2\pi f \tau_k} \quad (3)$$

In wideband channels, the difference between path delays $\{\tau_k\}$ can not be neglected. Therefore, a wideband channel undergoes frequency-selective multipath fading. The transfer function at one particular

frequency f_m is given by

$$\begin{aligned} H(f_m; t) &= \sum_{k=1}^L \alpha_k e^{j(2\pi f_k t + \phi_k)} e^{-j2\pi f_m \tau_k} \\ &= \sum_{k=1}^L \alpha_k(f_m) e^{j2\pi f_k t} = \sum_{k=1}^L \alpha_{mk} z_k^t \quad (4) \end{aligned}$$

where $e^{-j2\pi f_m \tau_k}$ and ϕ_k are absorbed into the complex gain α_{mk} , and $z_k = e^{j2\pi f_k}$. $\{z_k^T, k = 1, \dots, L\}$ are the so-called channel poles, where $1/T$ is the sampling rate. Although it requires a large L for $H(f_m; t)$ to experience Rayleigh fading, when deterministic Jakes model is used, the theoretical Doppler spectrum of the Rayleigh fading channel can be accurately approximated by a summation of a relatively small number of dominant (in terms of energy) sinusoids [8]. The parameters α_{mk} and f_k of these significant multipath components are assumed constant in the model, and they are estimated in order to predict the composite fading channel in future time. The Doppler frequency shift f_k is independent of f_m . Therefore, the Rayleigh time-variations of the channel transfer function at different frequencies are highly correlated, as they have the same channel poles. This fact enables us to collect the channel samples at different frequencies and estimate the channel poles jointly.

III. PARAMETER ESTIMATION

The channel estimation/prediction problem is now reduced to a classical frequency estimation problem, with an unknown number of Doppler frequencies closely spaced around zero. Subspace-based methods are characterized by their ability to resolve closely spaced sinusoids on the basis of short sample sequences. In this paper, we consider an ESPRIT-type method to estimate the channel poles associated with D dominant sinusoids. When estimating channel parameters with the ESPRIT algorithm, the number of channel poles that can be resolved is limited by the number of channel samples in the analysis segment and the number of frequency points we choose from the entire wideband. However, near-optimum performance can be achieved if D is chosen large enough [5].

A. Estimation of Channel Poles

From (4), the discrete-time channel transfer function at frequency f_m can be expressed as

$$\mathbf{H}_m = \mathbf{Z} \alpha_m + \eta_m \quad (5)$$

where

$$\mathbf{H}_m = \begin{bmatrix} H(f_m; 0) \\ H(f_m; T) \\ \vdots \\ H(f_m; (N-1)T) \end{bmatrix} \quad (6)$$

$$\mathbf{Z} = \begin{bmatrix} 1 & 1 & \cdots & 1 \\ z_1^T & z_2^T & \cdots & z_D^T \\ \vdots & \vdots & & \vdots \\ z_1^{(N-1)T} & z_2^{(N-1)T} & \cdots & z_D^{(N-1)T} \end{bmatrix} \quad (7)$$

$$\alpha_m = [\alpha_{m1} \ \alpha_{m2} \ \cdots \ \alpha_{mD}]' \quad (8)$$

η_m is the noise contribution, and superscript $'$ denotes the vector transpose operator. The observation interval is $[0, (N-1)T]$. Hereafter, we assume $T = 1$ in the analysis. Defining \mathbf{Z}^\downarrow (\mathbf{Z}^\uparrow) as the matrix \mathbf{Z} with the top (bottom) row deleted, we can write

$$\mathbf{Z}^\uparrow \Upsilon = \mathbf{Z}^\downarrow \quad (9)$$

where

$$\Upsilon = \text{diag}\{z_1, z_2, \dots, z_D\} \quad (10)$$

Collecting the channel transfer function samples in the observation interval at M frequency points within the wideband, we form the data matrix \mathbf{H} as

$$\mathbf{H} = [\mathcal{H}_0 \ \mathcal{H}_1 \ \cdots \ \mathcal{H}_{M-1}] \quad (11)$$

\mathcal{H}_m is an $L \times K$ Hankel matrix associated with the channel transfer function at frequency f_m

$$\mathcal{H}_m = \begin{bmatrix} H_m(0) & H_m(1) & \cdots & H_m(K-1) \\ H_m(1) & H_m(2) & \cdots & H_m(K) \\ \vdots & \vdots & & \vdots \\ H_m(L-1) & H_m(L) & \cdots & H_m(N-1) \end{bmatrix} \quad (12)$$

where $K + L = N + 1$. We need $L \geq KM$ to ensure that \mathbf{H} is of full column rank. Thus, K is chosen as

$$K = \lfloor \frac{N+1}{M+1} \rfloor \quad (13)$$

A subspace decomposition can be performed on \mathbf{H} by singular value decomposition (SVD) as

$$\mathbf{H} = [\mathbf{U}_s \ \mathbf{U}_n] \begin{bmatrix} \Sigma_s & \mathbf{0} \\ \mathbf{0} & \Sigma_n \end{bmatrix} \begin{bmatrix} \mathbf{V}_s^H \\ \mathbf{V}_n^H \end{bmatrix} \quad (14)$$

where $\mathbf{U}_s \in \mathcal{C}^{L \times D}$, $\Sigma_s \in \mathcal{R}^{D \times D}$, $\mathbf{V}_s \in \mathcal{C}^{KM \times D}$, and superscript H denotes Hermitian transpose operator. The orthonormal columns in \mathbf{U}_s associated with the D largest eigenvalues corresponding to the dominant sinusoids span the D -dimensional signal subspace. Therefore, in the following expression

$$\mathbf{U}_s^\uparrow \Phi = \mathbf{U}_s^\downarrow \quad (15)$$

matrix Φ is similar to matrix Υ . So Φ and Υ have the same eigenvalues, which are the channel poles. The least squares estimate of Φ is given by

$$\hat{\Phi} = (\mathbf{U}_s^\uparrow H \mathbf{U}_s^\uparrow)^{-1} \mathbf{U}_s^\uparrow H \mathbf{U}_s^\downarrow \quad (16)$$

The channel poles are projected onto the unit circle in accordance with the far-field channel model.

B. Estimation of Complex Path Gains

Based on the estimates of the channel poles $\{z_k\}$, the complex path gains α_m at each frequency can be determined by solving a set of linear equations as in (5). The least squares solution is given by

$$\hat{\alpha}_m = (\mathbf{Z}^H \mathbf{Z})^{-1} \mathbf{Z}^H \mathbf{H}_m \quad (17)$$

C. Channel Prediction and Performance Analysis

Once the channel poles and complex path gains are estimated, we can predict the channel transfer function $H(f_m; t)$ at future time from (4) for $t = NT, (N+1)T, \dots$. The prediction error $e_m(k)$ ($k = N, N+1, \dots$) is defined as the amplitude of the differences between predicted and actual channel samples

$$e_m(k) = |\hat{H}(f_m; kT) - H(f_m; kT)| \quad (18)$$

The performance of channel prediction is evaluated by the ratio of $e_m(k)$ to the root-mean-square (RMS) value of the envelope of the channel transfer function at frequency f_m . As a measure of prediction quality, we use the *prediction distance* defined in [2], for which the predicted and actual channels start to depart as this ratio becomes more than 20%. The prediction distance is converted to units of carrier wavelength λ in the simulation so that it is independent of the mobile speed.

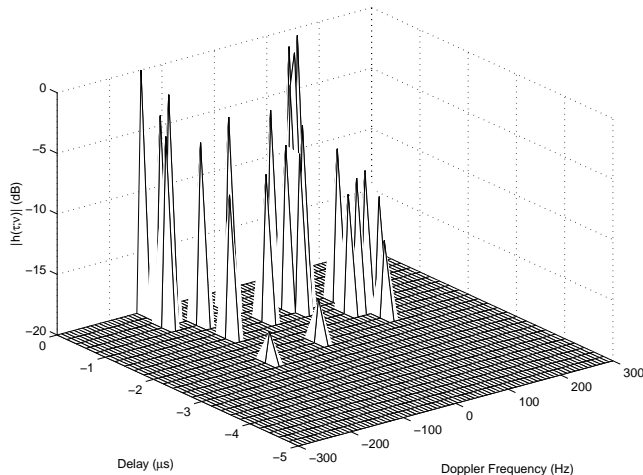


Fig. 1. Channel impulse response.

IV. SIMULATION

A wideband wireless system is simulated, in which the BS communicates with a mobile moving at a speed of 80 km/h. The carrier frequency is $f_c = 2$ GHz. Assume that the scatterers are uniformly distributed around the mobile. There are L significant multipath signals arriving at the BS, with the weakest having an amplitude no less than 20 dB lower than the amplitude of the most powerful one. The shortest multipath being as the reference, the propagation delay lengths and the phase offsets of the others are uniformly distributed on $[0 \text{ m}, 1000 \text{ m}]$ and $[0, 2\pi)$, respectively.

Fig. 1 illustrates the channel impulse response $h(\tau; \nu)$ in the domains of delay and Doppler frequency as

$$h(\tau; \nu) = \sum_{k=1}^L \alpha_k \delta(\nu + f_k) \delta(\tau - \tau_k) \quad (19)$$

The figure shows $L = 25$ significant multipath components with no more than 20 dB variation. The maximum Doppler frequency shift is limited by the mobile speed. Performing the 2-dimensional FFT on $h(\tau; \nu)$ results in the time-varying channel transfer function $H(f; t)$. Fig. 2 illustrates the baseband channel transfer function spanning a bandwidth of 5 MHz. The channel experiences fast fading and there are deep fades within a time frame of 10 ms.

The channel transfer function is sampled at $M = 32$ evenly spaced frequency points within the 5 MHz

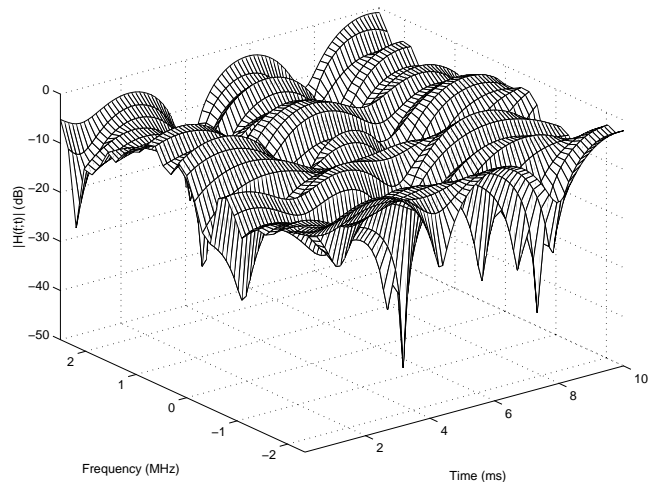


Fig. 2. Channel transfer function.

band. An example of channel prediction is demonstrated in Fig. 3, which shows the amplitudes and phases of the channel transfer functions at the fourth and twelfth frequency points. The region to the left of the vertical line is the observation interval as the analysis segment, and the region to the right is the prediction segment. The observation interval is $[0, 3.9 \text{ ms}]$, which is $[0, 0.58\lambda]$ in wavelength units. At each frequency, 32 channel samples in the observation interval are used. Note that the sampling rate is higher than the Nyquist rate, which is twice the maximum Doppler frequency. It does not benefit by sampling the channel as densely as the data rate, because the channel variation is characterized by the Doppler frequencies. The Doppler frequencies $\{f_k\}$ are limited to a few hundred hertz, and T takes up only a few milliseconds, therefore the channel poles $\{z_k^T = e^{j2\pi f_k T}\}$ condense near 1 in the complex plan. There are $L = 100$ significant multipath components with 20 dB variation range. The channel output SNR is fixed at 20 dB. We choose $D = 12$. Channel poles with amplitude larger than 1.1 or smaller than 0.9 are discarded, since they are usually not related to the Doppler frequencies of the channel. And the remaining poles are projected onto the unit circle.

Fig. 4 and Fig. 5 make the performance comparison between the joint-frequency channel prediction and the prediction conducted at each frequency individually, with the channel output SNR varying from 0 to 40 dB. The observation intervals are chosen as $[0, 0.58\lambda]$, $[0, 2.31\lambda]$ and $[0, 4.63\lambda]$, and a fixed num-

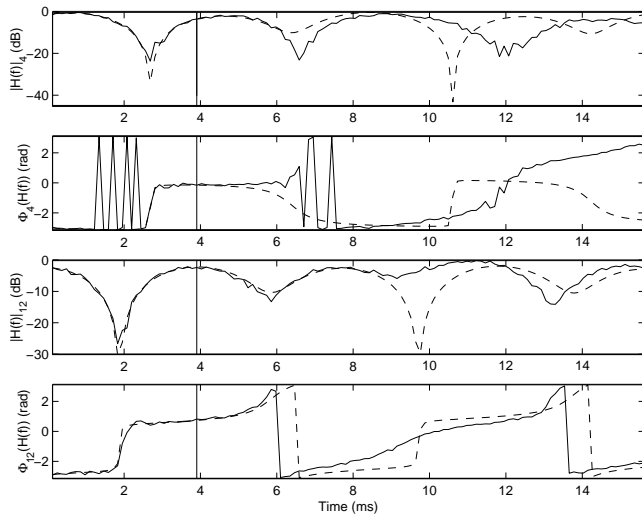


Fig. 3. Channel prediction example. (— : actual channel, ··· : predicted channel.)

ber of 32 samples are taken from each interval. There are $L = 10$ significant multipath components simulated in Fig. 4, and $L = 100$ in Fig. 5. The number of Monte Carlo trials is 200. Because the joint-frequency wideband channel prediction uses more data in the observation interval to estimate the channel poles, it provides better prediction performance.

V. CONCLUSION

Prediction of the frequency-selective fading channel in the wideband systems has been investigated in a fast fading environment. The simulations use a static model with far-field scatterers and constant mobile velocity. Applying the subspace method jointly at different frequencies within the wideband offers reliable prediction of the channel transfer function. The proposed prediction algorithm outperforms the channel prediction over a single frequency with an observation interval of the same length.

REFERENCES

- [1] A. Duel-Hallen, S. Hu and H. Hallen, "Long-range prediction of fading signals," *IEEE Signal Processing Mag.*, vol. 17, no. 3, pp. 62–75, May 2000.
- [2] R. Vaughan, P. Teal and R. Raich, "Short-term mobile channel prediction using discrete scatterer propagation model and subspace signal processing algorithms," in *Proc. VTC*, Sept. 2000, pp. 751–758.
- [3] T. Eyceoz, A. Duel-Hallen and H. Hallen, "Deterministic channel modeling and long range prediction of fast fading

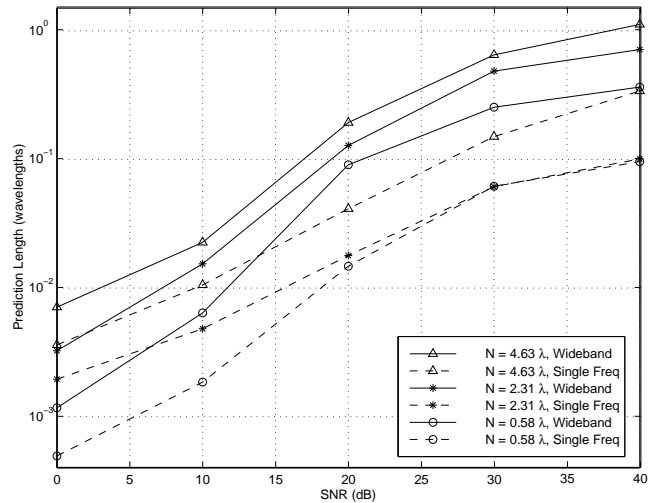


Fig. 4. Channel prediction performance, $L = 10$.

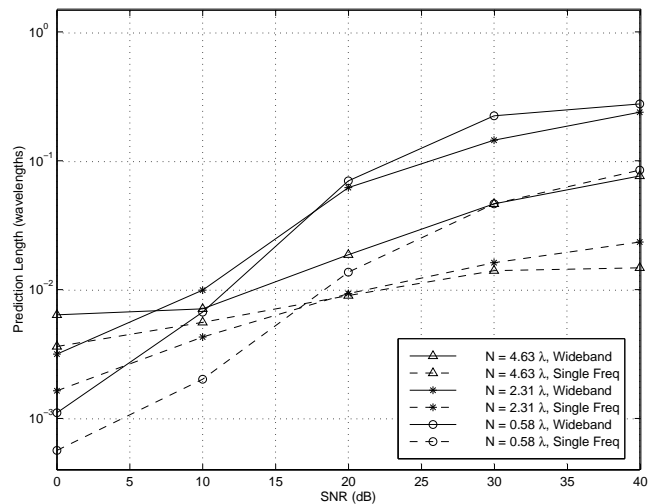


Fig. 5. Channel prediction performance, $L = 100$.

mobile radio channels," *IEEE Commun. Lett.*, vol. 2, pp. 254–256, Sept. 1998.

- [4] J. Hwang and J. Winters, "Sinusoidal modeling and prediction of fast fading processes," in *Proc. GLOBECOM*, Nov. 1998, pp. 892–897.
- [5] J. Andersen, J. Jensen, S. Jensen and F. Frederiksen, "Prediction of future fading based on past measurements," in *Proc. VTC*, Sept. 1999, pp. 151–155.
- [6] T. Ekman and G. Kubin, "Nonlinear prediction of mobile radio channels: measurements and MARS model designs," in *Proc. ICASSP*, May 1999, vol. 5, pp. 2667–2670.
- [7] R. Roy and T. Kailath, "ESPRIT – estimation of signal parameters via rotational invariance techniques," *IEEE Trans. Acoust., Speech, Signal Processing*, vol. 37, no. 7, pp. 984–995, July 1989.
- [8] W. C. Jakes, *Microwave Mobile Communications*, John Wiley and Sons, New York, 1974.